

ANALYSIS OF WIND ENERGY CONVERSION SYSTEM EMPLOYING DFIG WITH SPWM AND SVPWM TYPE CONVERTERS

G.PANDU RANGA REDDY¹

Dr.M.VIJAYA KUMAR²

¹G.P.C.E.T, Kurnool, A.p, gprreee@gmail.com

²J.N.T.U.C.E, Anantapur, A.p, mvk_2004@reddiffmail.com

Abstract:

Renewable energy is catching people's attention with increasing global energy consumption and noticeable environmental pollution across the globe. Wind energy is the one of the most available and exploitable forms of renewable energy. Winds blow from a region of higher atmospheric pressure to one of lower atmospheric pressure. In variable-speed wind turbines grid synchronization is possible at any operational speed. For this, it is necessary to operate the converter station with effective modulation technique. This paper presents the analysis of variable speed wind energy conversion system employing double fed induction generator with SPWM and SVPWM type converters. The MATLAB/SIMULINK software is used for simulating the models.

Key words: Double fed induction generator, Rectifier, Inverter, PWM, SVPWM, Wind Turbine.

1. Introduction

Renewable energy including solar, wind, tidal, small hydro geothermal, refused derived fuel and fuel cell energies is sustainable, reusable and environmentally friendly and clean. With the increasing shortage in fossil fuels, and pollution problems renewable energy has become an important energy source. Among the other renewable energy sources wind energy has proven to be one of the most economical one, because it is considered to be nonpolluting and economically viable. At the same time, there has been a rapid development of related wind turbine technology [1].

As far as variable-speed generation is concerned, it is necessary to produce constant-frequency electric power from a variable speed source. This can be achieved by means of synchronous generators, provided that a static frequency converter is used to interface the machine to the grid. An alternative approach consists in using a wound-rotor induction generator fed with variable frequency rotor voltage. This allows fixed-frequency electric power to be extracted from the generator stator.

When used with a wind turbine it offers several advantages over the fixed speed generator systems. These advantages, including speed control and reduced flickers, are primarily achieved by controlling the voltage source converter, with its inherent bidirectional active and reactive power flow [2]. The DFIG using back-to-back

PWM converters for the rotor-side control has been well established in wind power system.

Consequently, the use of doubly fed induction machines is receiving increasing attention for wind generation purposes [1]. The stator of DFIG is directly connected to the power grid, and the rotor windings are supplied from back-to-back voltage source converters (VSC) via slip rings. Fig.1. shows the schematic diagram of WT with DFIG connected to an infinite bus [2].

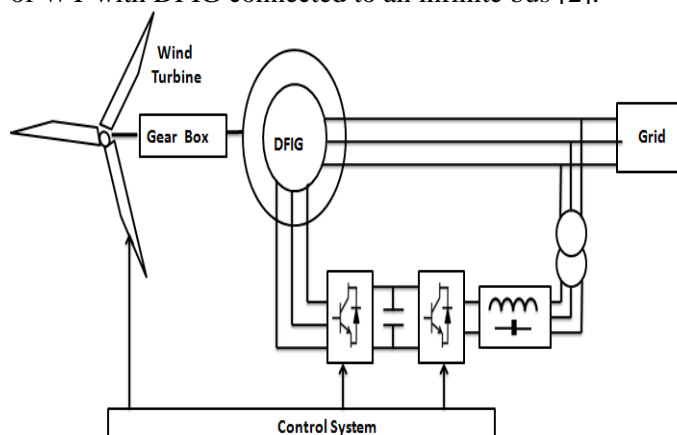


Fig 1. DFIG based wind turbine scheme

Wind turbine converts the kinetic energy of the wind into electric energy. Torque is generated by the aerodynamic lift force of turbine's blades, and transferred to the rotor shaft. In this way, the linear kinetic energy of the wind (P_w) is converted into rotational energy of the turbine shaft (P_m) connected to the same shaft, the electric generator converts mechanical rotational energy into electrical energy (P_e). A rectifier is used to convert the electrical alternating current (AC) into electrical direct current (DC), while inverter converts it from DC to AC, providing power to grid [3].

In view of this the paper is organized as follows: Section 2 deals with the dynamic modeling of wind turbine, DFIG modeling and the modeling of voltage source converters. The modulation techniques used to operating the proper switching of the voltage source converters has been explained in section 3. The simulation results of DFIG based WECS with SPWM and SVPWM have been shown in section 4 and the conclusions are presented in section 5.

2. Designing of Wind Energy Conversion System:

2.1. Wind Turbine modeling:

The Mechanical power captured from the wind and the mechanical torque developed by the turbine shaft can be calculated using the well-known aerodynamic Equations (1) and (2) [2].

$$P_m = \frac{1}{2} \rho C_p(\lambda, \beta) A_r V_w^3 \quad (1)$$

$$T_m = \frac{P_m}{\omega_r} = \frac{1}{2} \rho C_p(\lambda, \beta) A_r V_w^2 \frac{R_r}{\lambda} \quad (2)$$

The power coefficient (C_p) indicates how efficiently the conversion of wind power to rotational mechanical power is performed by the wind turbine. It is a function of TSR (Tip – Speed Ratio, λ) and the rotor blade pitch angle (β) according to equation(3).

$$C_p(\lambda, \beta) = 0.73 \left(\frac{151}{\lambda_i} - 0.58\beta - 0.002\beta^{2.14} - 13.2 \right) e^{\frac{-18.4}{\lambda_i}} \quad (3)$$

Where

$$\lambda_i = \frac{1}{\frac{1}{\lambda - 0.02\beta} - \frac{0.003}{\beta^3 + 1}} \quad (4)$$

And

$$\text{TSR}(\lambda) = \frac{\omega_r R_r}{V_w} \quad (5)$$

The theoretical limit for C_p is 0.59 according to Benz's Law but its practical range of variation is 0.2 – 0.4. In this paper, the rotor pitch angle is assumed to be fixed.

The wind turbine is normally characterized by $P_m - \omega_r$ and $C_p - \lambda$ curves as illustrated in Fig. 2. The turbine power (P_m) is determined from the power conversion coefficient (C_p) and TSR (λ). If the swept area, air density, and wind speed are constant. The power conversion coefficient and TSR depend on the aerodynamic characteristics of wind turbine. From Fig. 2, the maximum turbine power is found at point λ_{opt} and C_{pmax} [1].

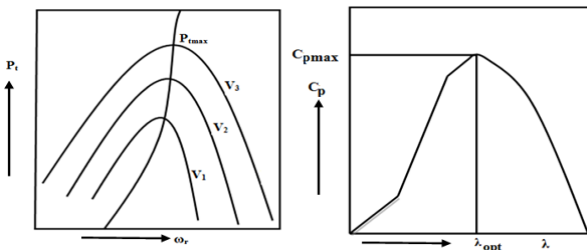


Fig 2. Wind turbine charecteristic.
(a) $P_m - \omega_r$ Curve (b) $C_p - \lambda$ Curve

The matlab/simulink diagram of wind turbine system as shown in Fig 3.

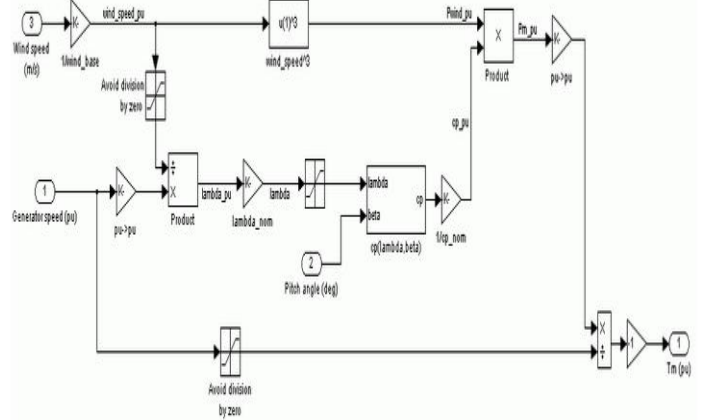


Fig 3.Simulation diagram for wind turbine.

2.2. Dynamic modeling of double fed induction generator (DFIG):

The DFIG model using d-q synchronous reference frame is being presented here with the equations, Modeling can be of different type depending upon the type of study but basically modeling consists of the mathematical equations of DFIG which can be achieved from the equivalent circuit of the DFIG [5].

The equivalent circuit of the DFIG, including the magnetic losses, can be seen in Fig.4. This equivalent circuit is valid for one equivalent Y phase and for steady-state with the $j\omega$ method for calculations [6].

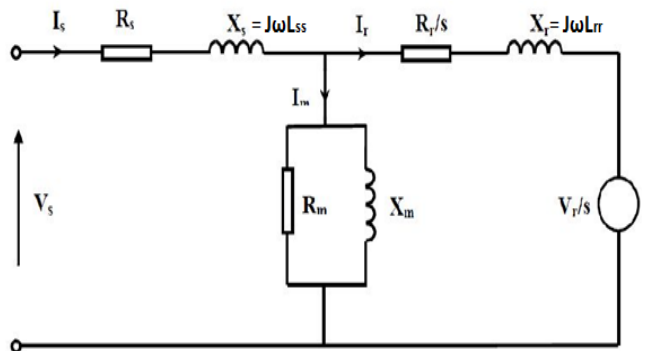


Fig 4. Equivalent circuit of DFIG Machine

For balanced steady state conditions the d and q variables are sinusoidal in all reference frames except the synchronously rotating reference frame wherein they are constants for synchronously rotating reference frame. The d – q components of voltages are described as follows [8]:

$$V_{ds} = R_s i_{ds} + \frac{d\psi_{ds}}{dt} - \omega_s \psi_{qs} \quad (6)$$

$$V_{qs} = R_s i_{qs} + \frac{d\psi_{qs}}{dt} + \omega_s \psi_{ds} \quad (7)$$

$$V_{dr} = R_s i_{dr} + \frac{d\psi_{dr}}{dt} - (\omega_s - \omega_r) \psi_{qr} \quad (8)$$

$$V_{qr} = R_s i_{qr} + \frac{d\psi_{qr}}{dt} + (\omega_s - \omega_r) \psi_{dr} \quad (9)$$

The ψ stands for flux linkage and express as:

$$\psi_{ds} = L_{ss} i_{ds} + L_m i_{dr} \quad (10)$$

$$\psi_{qs} = L_{ss} i_{qs} + L_m i_{qr} \quad (11)$$

$$\psi_{dr} = L_{rr} i_{dr} + L_m i_{ds} \quad (12)$$

$$\psi_{qr} = L_{rr} i_{qr} + L_m i_{qs} \quad (13)$$

and also

$$L_{ss} = L_s + L_m \quad (14)$$

$$L_{rr} = L_r + L_m \quad (15)$$

For a simple mechanical system of moment of inertia J and damping factor F , the rotor swing equation is

$$J \frac{d\omega_{rm}}{dt} + F\omega_{rm} = (T_e - T_m) \quad (16)$$

Where

ψ_s , i_s and Ψ_s are stator voltage, current and flux respectively;

λ_r , i_r and Ψ_r are rotor voltage, current and flux respectively;

ω_s and ω_r are the angular velocity of the chosen frame of reference;

ω_{rm} represents the mechanical speed of rotor;

d and q represents the d and q axis, respectively;

L_m is the mutual inductance;

L_{ss} and L_{rr} are the stator and rotor self inductances, respectively;

T_m is representing mechanical torque;

T_e represents electrical torque.

2.3. Back-to-back VSC Converters:

A back-to-back voltage source converter (VSC) consists of two converters, i.e., generator-side converter called the rectifier and the grid-side converter called the inverter with a DC-link capacitor which is placed between these two converters. These two bidirectional VSCs connecting through the rotor of the generator and the grid as shown in Fig 1. Basically these converters are made up of insulated gate bipolar transistor (IGBT) switches which permit a bidirectional current flow [7].

The main objective for the grid-side converter is to keep the variation of the DC-link voltage is small. Output switching harmonics of the grid side converter is diminished by the filters. The generator-side converter is used to control the torque, the speed of a DFIG as well as its active and reactive power at the stator terminals [4].

2.3.1 Generator-side Converter Control:

The main purpose of the generator side converter is to maintain the rotor speed constant irrespective of the wind speed and also the control strategy has been implemented to control the active power and reactive power flow of the machine using the rotor current components. The active power flow is controlled through i_{dr} and the reactive power flow is controlled through i_{qr} [9]. The generator-side converter controller is also used to regulating the torque developed in the rotor of the DFIG. It acts as a rectifier as shown in Fig. 5 for converting the unregulated generated alternate power into direct power.

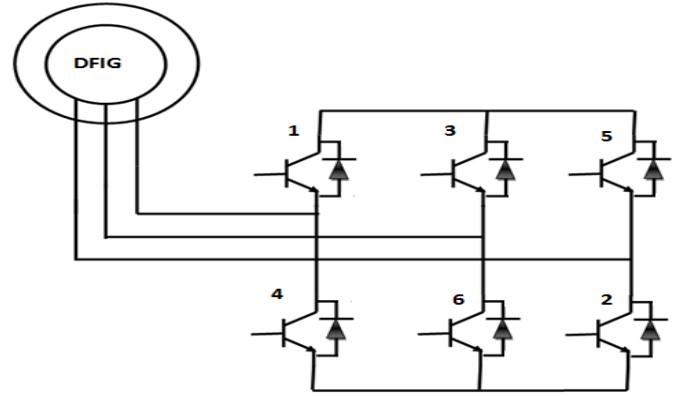


Fig 5. Three Phase AC/DC Converter

2.3.2 Grid-side Converter Control:

The objective of the grid-side converter is to keep the DC-link voltage constant regardless of the magnitudes of the grid-side voltages, and to yield a unity power factor looking into the WTGS from the grid-side [7]. It acts as a DC-to-AC inverter. The DC-to-AC inverter is used for many applications including motor drives, uninterruptable power supplies, aircraft power, lagging and leading varies generation, and on renewable energy (solar, wind, fuel-cells, small hydro, etc.) systems. This type of converter produces a sinusoidal ac output waveform whose magnitude and frequency can be controlled. They are used to deliver power from a dc source, such as a battery, to a passive or active ac load using semiconductor devices, such as SCRs or gate driven devices including GTOs, IGBTs, and MOSFETs. Due to the advance in semiconductor devices, today's switches have higher switching frequencies and more power capabilities together with improved control techniques. Due to this the inverter can operate in a wide range of regulated output voltage and frequency with reduced harmonics. The Fig.6 shows the three Phase DC/AC converter [10].

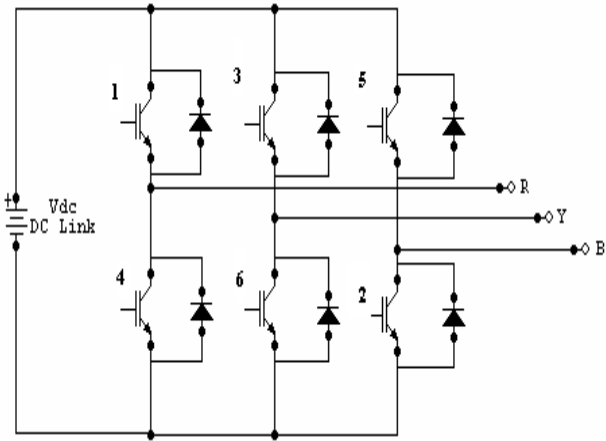


Fig 6. Three Phase DC/AC Converter

Gating signals for the converter devices are generated by employing a sinusoidal pulse width modulation technique (SPWM) and space vector pulse width modulation techniques (SVPWM).

3. Modulation Techniques for Converters:

3.1. SPWM technique:

The sinusoidal pulse width modulation (SPWM) is the most widely used PWM technique for converters of two and more levels. It mainly controls the width of pulse and its main use is to allow the control of the power supplied to electrical devices especially to inertial loads such as motors. The basic principle of the SPWM is explained here. The reference signal (V_r) is the generally sinusoidal signal and is compared with the high frequency triangle wave called the carrier wave (V_c) of constant amplitude. When $V_r > V_c$, the PWM output will be high (state +1), and the output will be low (state -1) for $V_r < V_c$ as shown in Fig.7.

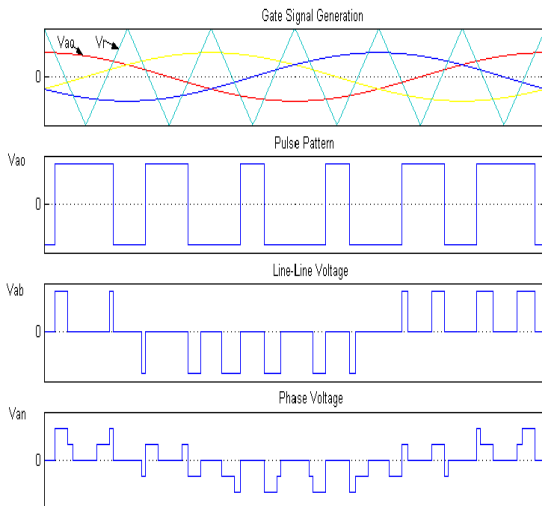


Fig 7. Three phase sinusoidal PWM

The advantages possessed by PWM techniques are

- This method can be obtained without any additional components.
- In this method, lower order harmonics can be eliminated or minimized along with its output voltage control. As higher order harmonics can be filtered easily, the filtering requirements are minimized.

The main disadvantage of this method is that SCRs are expensive as they must possess low turn-on and turn-off times. The three-phase PWM rectifier is a boost converter due to the following equation [16]

$$V_{dc} \propto \frac{\sqrt{2}V_a}{M_i} \quad (17)$$

In general the modulation index is defined as the ratio of the magnitude of the reference signal to that of the carrier signal. The modulation index can be given by the following relation

$$M_i = \frac{V_r}{V_c} \quad (18)$$

Where

V_r is the magnitude of the sinusoidal reference signal waveform and

V_c is the magnitude of the triangular carrier signal waveform

By varying V_r and keeping V_c constant, the modulation can be changed. By changing the modulation index, the amplitude of the fundamental component of the output can be varied. For three phase inverters, the same carrier signal V_c is used for all the three phases and three reference signals which are phase displaced by $2\pi/3$ radians are used for each of the phases.

3.2. SVPWM technique:

The space vector concept, which was originally derived from the rotating field of induction motors, is used in the application of pulse width modulation [4]. Space vector pulse width modulation (SVPWM) is a more sophisticated technique for generating modulation signals, and it has many advantages when compared with the conventional SPWM techniques. Those are 1) reduced commutation losses 2) higher amplitude of the modulation index, 3) greater DC-bus voltage utilization, and 4) lower the total harmonic distortion (THD) of the output voltages.

In this modulation technique the three phase quantities can be transformed to their equivalent two-phase quantity either in synchronously rotating frame (or) stationary frame. From these two-phase components, the reference vector magnitude can be found and used for modulating the inverter output.

Considering the stationary reference frame let the three-phase sinusoidal voltage component be [13],

$$V_R = V_m \sin \omega t \quad (19)$$

$$V_Y = V_m \sin(\omega t - \frac{2\pi}{3}) \quad (20)$$

$$V_B = V_m \sin(\omega t - \frac{4\pi}{3}) \quad (21)$$

When this three-phase voltage is applied to the AC machine it produces a rotating flux in the air gap of the AC machine. This rotating resultant flux can be represented as single rotating voltage vector. The magnitude and angle of the rotating vector can be found by means of Clark's Transformation.

Space Vector PWM (SVPWM) refers to a special switching sequence of the upper three power transistors of a three-phase power inverter. It has been shown to generate less harmonic distortion in the output voltages and/or currents applied to the phases of an AC motor and to provide more efficient use of dc input voltage [12].

The circuit schematic of a typical three-phase voltage source PWM inverter is shown in Fig 6. The six power switches, 1 to 6, shape the output voltages. The switches must be controlled so that at no time are both switches in the same leg turned on or else the DC supply would be shorted.

$$S_K = \begin{cases} 1 & \text{The upper IGBT is ON} \\ 0 & \text{The lower IGBT is ON} \end{cases} \quad (22)$$

For each phase, there will be two switching states. As a result, there are $2^3=8$ possible switching patterns for the three-phase two-level inverter.

Fig.8 shows the basic switching Vector of SVPWM technique. In this scheme there are eight valid switching states out of six active switching space vectors are evenly distributed 60° interval with $2V_{dc}/3$ length and form a hexagon [14].

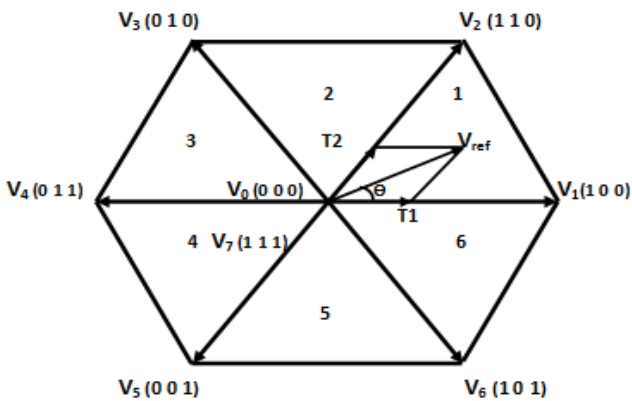


Fig 8.Space vector diagram with sectors

The non-zero vectors can be represented by the following equation [11]:

$$V_k = \frac{2}{3} V_{dc} e^{j(k-1)\frac{\pi}{3}} \quad \text{Where } k=1,2,\dots,6 \quad (23)$$

Also two zero space vectors are located at the center of hexagon in the complex plane as shown in Fig.6. For a given Magnitude (length) and position, V_{ref} can be synthesized by three nearby stationary vectors, based on which the switching states of the inverter can be selected and gate signals for the active switches can be generated. The reference vector is sampled at equal intervals of time, referred to as sampling time period [12].

Table 1.Switching Pattern of active switching states

Angle	Sector	X	Y	Z _x	Z _y
0 - 60	I	1	2	0	7
60 - 120	II	2	3	7	0
120 - 180	III	3	4	0	7
180 - 240	IV	4	5	7	0
240 - 300	V	5	6	0	7
300 - 360	VI	6	1	7	0

3.2.1 Steps for implementing the space vector PWM:

The space vector PWM can be implemented by the following steps [15]:

Step 1. Determine V_d , V_q , V_{ref} , and angle (α).

Step 2. Determine time duration T_1 , T_2 , T_0 .

Step 3. Determine the switching time of each transistor (S_1 to S_6).

Step-1: Determine, V_d , V_q , V_{ref} and angle (α):

From the Fig.9, V_d , V_q , V_{ref} and angle (α) can be determined as follows:

$$V_d = V_{an} - V_{bn} \cos 60^\circ - V_{cn} \cos 60^\circ \quad (24)$$

$$= V_{an} - V_{bn} \frac{1}{2} - V_{cn} \frac{1}{2}$$

$$V_q = 0 + V_{bn} \cos 30^\circ - V_{cn} \cos 30^\circ \quad (25)$$

$$= 0.V_{an} + V_{bn} \frac{\sqrt{3}}{2} - V_{cn} \frac{\sqrt{3}}{2}$$

$$\therefore \begin{bmatrix} V_d \\ V_q \end{bmatrix} = \begin{bmatrix} 1 & -\frac{1}{2} & -\frac{1}{2} \\ 0 & \frac{\sqrt{3}}{2} & -\frac{\sqrt{3}}{2} \end{bmatrix} \begin{bmatrix} V_{an} \\ V_{bn} \\ V_{cn} \end{bmatrix}$$

$$\therefore |V_{ref}^-| = \sqrt{(V_d)^2 + (V_q)^2}$$

$$\alpha = \tan^{-1}\left(\frac{V_d}{V_q}\right) = \omega t = 2\pi f t$$

Where f = fundamental frequency.

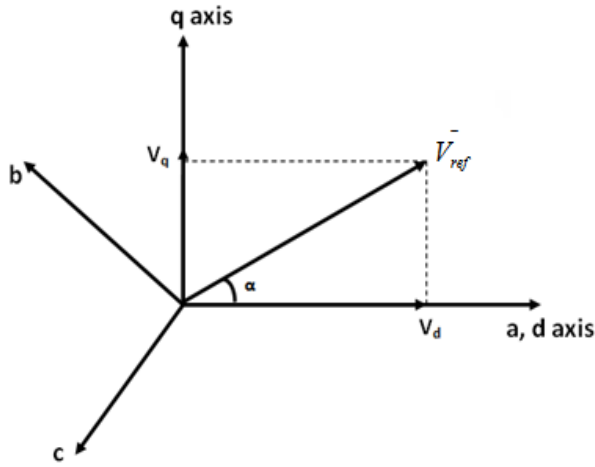


Fig 9. Voltage space vector and its components in (d,q)

Step-2: Determine the time duration T_1 , T_2 and T_0 :

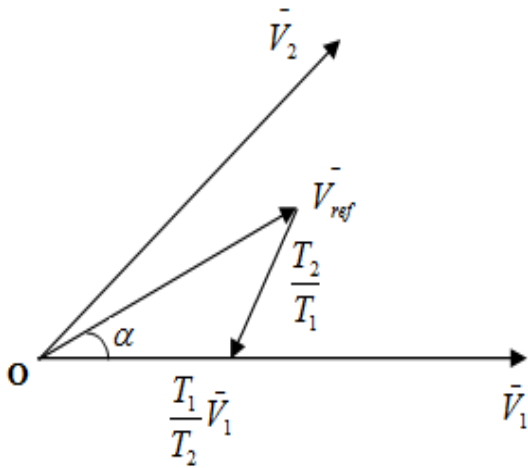


Fig 10. Reference vector as a combination of adjacent vectors.

From the Fig.10 the switching time duration can be calculated as follows

$$(26) \quad \int_0^{T_z} V_{ref}^- dt = \int_0^{T_1} V_1^- dt + \int_{T_1}^{T_1+T_2} V_2^- dt + \int_{T_1+T_2}^{T_z} V_0^- dt$$

$$(27) \quad \bar{V}_{ref} \angle \alpha^0 T_z = \frac{2}{3} V_{dc} \angle 0^0 T_1 + \frac{2}{3} V_{dc} \angle 60^0 T_2 \quad (29)$$

By performing algebraic operations

$$T_1 = T_z \cdot a \cdot \frac{\sin\left(\frac{\pi}{3} - \alpha\right)}{\sin\left(\frac{\pi}{3}\right)} \quad (30)$$

$$T_2 = T_z \cdot a \cdot \frac{\sin(\alpha)}{\sin\left(\frac{\pi}{3}\right)} \quad (31)$$

$$T_0 = T_z - (T_1 + T_2) \quad (32)$$

$$\text{Where } T_z = \frac{1}{f_z} \text{ and } a = \frac{|V_{ref}^-|}{\frac{2}{3} V_{dc}} \quad (33)$$

Switching time duration of any sector is

$$\therefore T_1 = \frac{\sqrt{3} T_z |V_{ref}^-|}{V_{dc}} \left(\sin\left(\frac{\pi}{3} - \alpha + \frac{n-1}{3} \pi\right) \right) \quad (34)$$

$$= \frac{\sqrt{3} T_z |V_{ref}^-|}{V_{dc}} \sin\left(\frac{n}{3} \pi - \alpha\right) \quad (35)$$

$$= \frac{\sqrt{3} T_z |V_{ref}^-|}{V_{dc}} \left(\sin \frac{n}{3} \pi \cdot \cos \alpha - \cos \frac{n}{3} \pi \sin \alpha \right) \quad (36)$$

$$\therefore T_2 = \frac{\sqrt{3} T_z |V_{ref}^-|}{V_{dc}} \left(\sin\left(\alpha - \frac{n-1}{3} \pi\right) \right) \quad (37)$$

$$= \frac{\sqrt{3} T_z |V_{ref}^-|}{V_{dc}} \left(-\cos \alpha \cdot \sin \frac{n-1}{3} \pi + \sin \alpha \cdot \cos \frac{n-1}{3} \pi \right) \quad (38)$$

$$\therefore T_0 = T_z - T_1 - T_2 \quad (39)$$

Where, n=1 through 6 (Sector 1 to 6) $0 \leq \alpha \leq 60^0$

Step-3: Investigate the switching time of each transistor:

Fig.11 shows space vector PWM switching patterns at each sector. Based on this the switching time at each sector is summarized in Table-2.

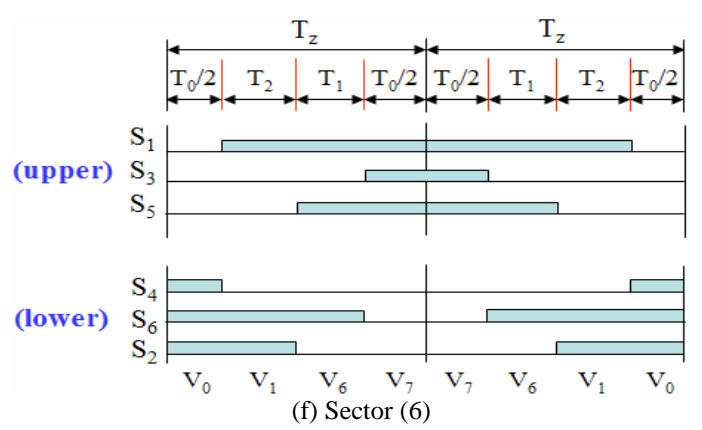
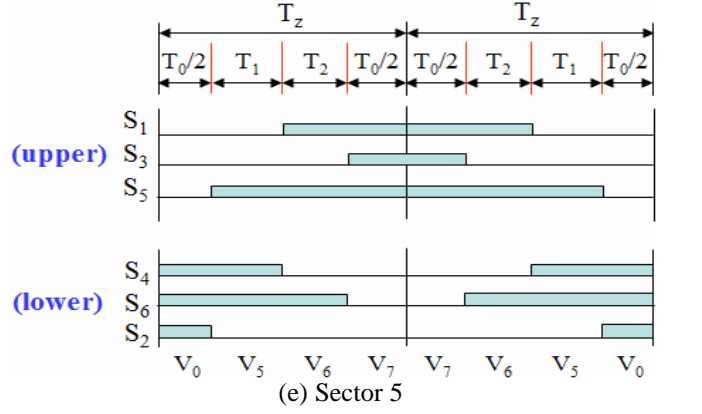
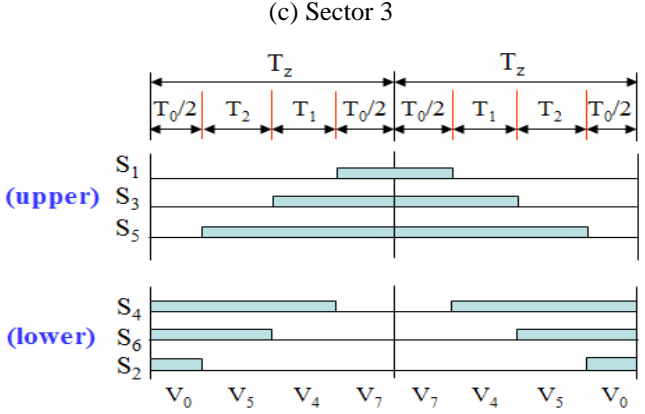
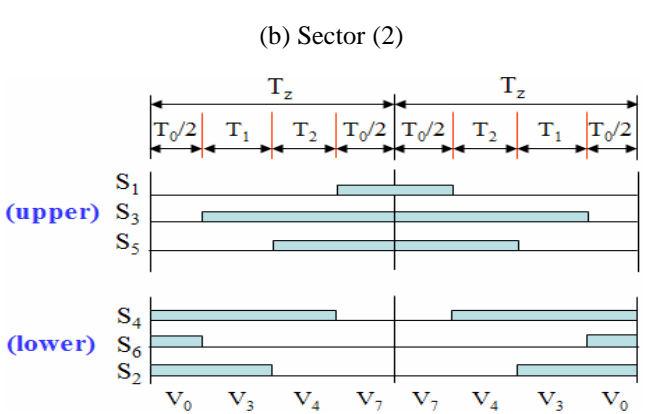
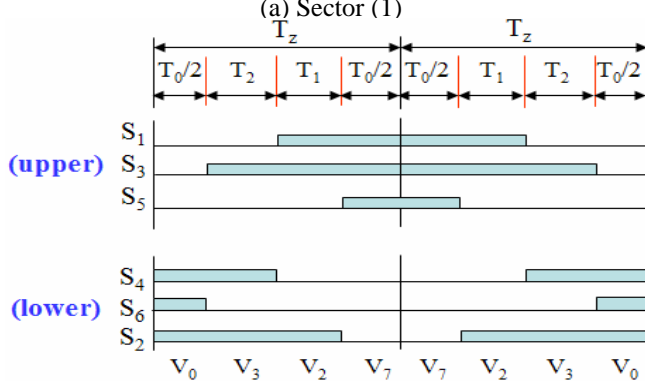
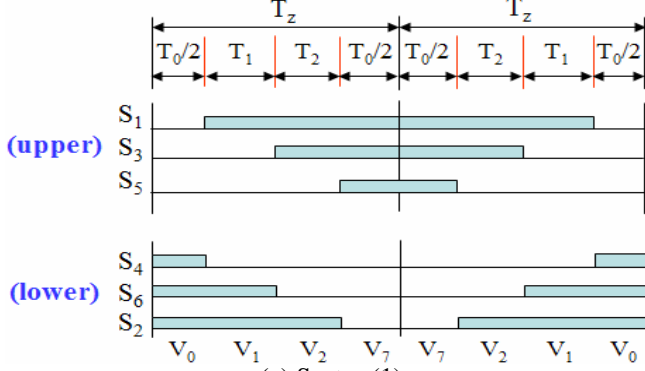


Fig 11. Switching pulse pattern for the three phases in the 6 different sectors.

Table.2 switching time calculation at each sector

Sector	Upper Switches (S1, S3, S5)	Lower Switches (S4, S6, S2)
1	$S_1 = T_1 + T_2 + \frac{T_0}{2}$ $S_3 = T_2 + \frac{T_0}{2}$ $S_5 = \frac{T_0}{2}$	$S_4 = \frac{T_0}{2}$ $S_6 = T_2 + \frac{T_0}{2}$ $S_2 = T_1 + T_2 + \frac{T_0}{2}$
2	$S_1 = T_1 + \frac{T_0}{2}$ $S_3 = T_1 + T_2 + \frac{T_0}{2}$ $S_5 = \frac{T_0}{2}$	$S_4 = T_2 + \frac{T_0}{2}$ $S_6 = \frac{T_0}{2}$ $S_2 = T_1 + T_2 + \frac{T_0}{2}$
3	$S_1 = \frac{T_0}{2}$ $S_3 = T_1 + T_2 + \frac{T_0}{2}$ $S_5 = T_2 + \frac{T_0}{2}$	$S_4 = T_1 + T_2 + \frac{T_0}{2}$ $S_6 = \frac{T_0}{2}$ $S_2 = T_1 + \frac{T_0}{2}$

4	$S_1 = \frac{T_0}{2}$ $S_3 = T_1 + \frac{T_0}{2}$ $S_5 = T_1 + T_2 + \frac{T_0}{2}$	$S_4 = T_1 + T_2 + \frac{T_0}{2}$ $S_6 = T_2 + \frac{T_0}{2}$ $S_2 = \frac{T_0}{2}$
5	$S_1 = T_2 + \frac{T_0}{2}$ $S_3 = \frac{T_0}{2}$ $S_5 = T_1 + T_2 + \frac{T_0}{2}$	$S_4 = T_1 + \frac{T_0}{2}$ $S_6 = T_1 + T_2 + \frac{T_0}{2}$ $S_2 = \frac{T_0}{2}$
6	$S_1 = T_1 + T_2 + \frac{T_0}{2}$ $S_3 = \frac{T_0}{2}$ $S_5 = T_1 + \frac{T_0}{2}$	$S_4 = \frac{T_0}{2}$ $S_6 = T_1 + T_2 + \frac{T_0}{2}$ $S_2 = T_1 + \frac{T_0}{2}$

4.Simulation results & Discussions:

The modulation technique main aim is to obtain variable output having maximum fundamental component with minimum harmonics. The objective of PWM techniques is to enhancement of fundamental output voltage and reduction of harmonic content in three phase voltage source inverters.

In this paper PWM & SVPWM techniques applied to DFIG based wind energy conversion system are compared in terms of Total Harmonic Distortion (THD). In this paper up to $t = 0.2$ sec the WECS is not connected to the grid. After $t = 0.2$ sec the WECS employing DFIG is connected to the grid. Simulink Models has been developed by using MATLAB software for SPWM and SVPWM techniques.

4.1. Simulation results using SPWM technique:

The following figures represent the simulation results of SPWM technique applied to DFIG based wind energy conversion system.

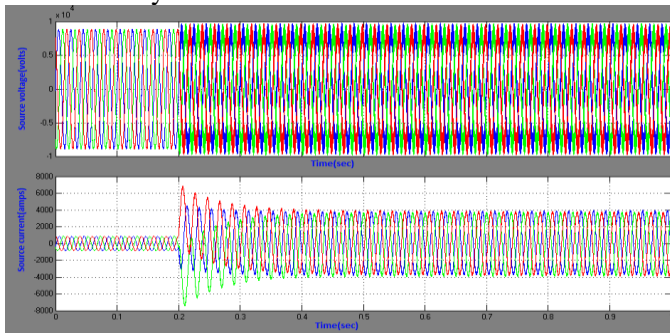


Fig 12.Source voltage and current of DFIG based WECS

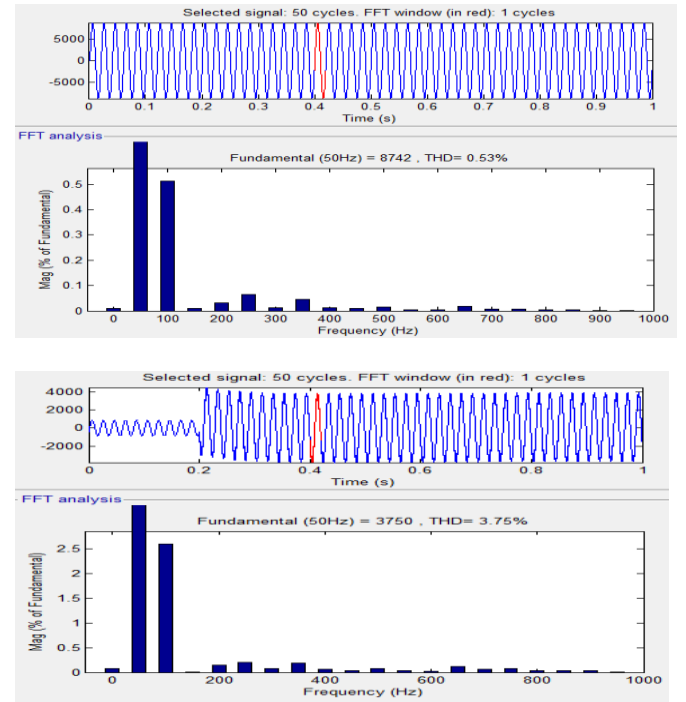


Fig 13.Source voltage and source current harmonic spectrum of two level VSC using SPWM

The simulation result of Fig.12 shows that, the voltage and current supplied by source. From Fig.13, the THD value of source voltage and source current for two level voltage source converter (VSC) using SPWM is 0.53% & 3.75% respectively.

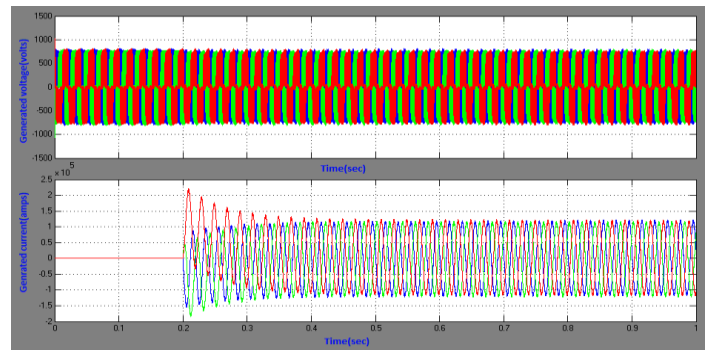
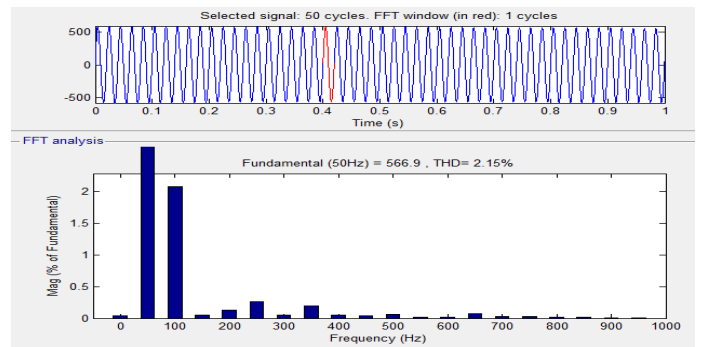


Fig 14.Generated voltage and current of DFIG



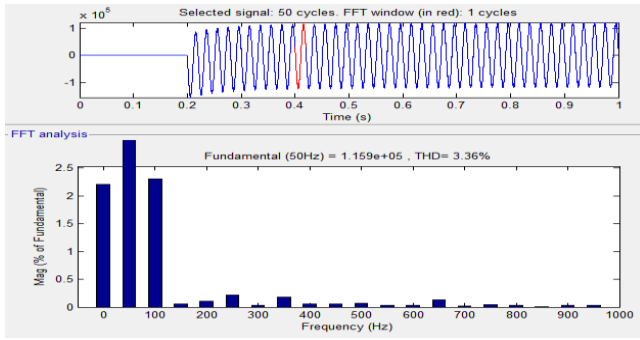


Fig 15. Generated voltage and current harmonic spectrum of two level VSC using SPWM

The Fig .14 shows the voltage and current generated by the DFIG machine. The current upto $t = 0.2$ sec is zero as DFIG is not connected to the load. After $t = 0.2$ sec DFIG generates current to the load. From Fig.15, the THD value of generated voltage and current for two level voltage source converter(VSC) using SPWM is 2.15% & 3.36% respectively.

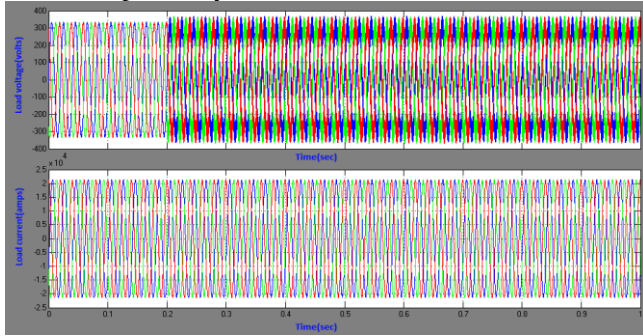


Fig 16. Load voltage and current of DFIG based WECS.

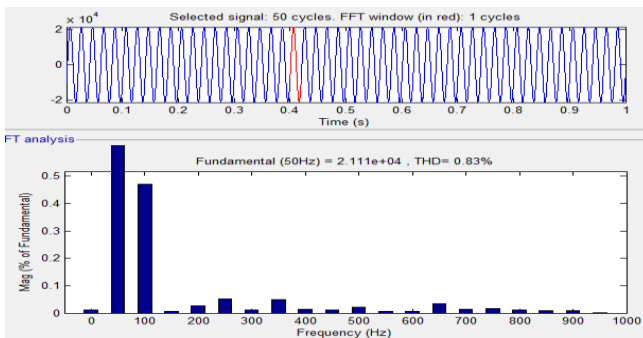
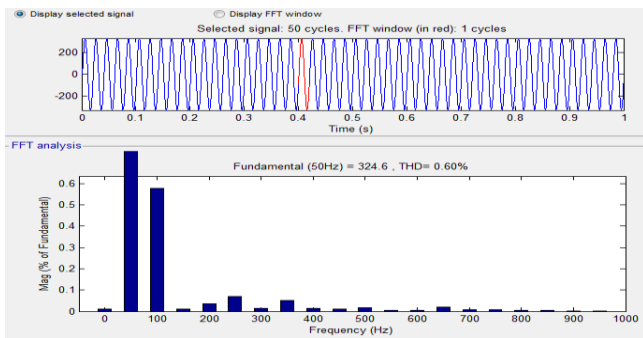


Fig 17. Load voltage and current harmonic spectrum of two level VSC using SPWM

The Fig. 16 shows the voltage and current received by the load. Here the voltage and current after $t = 0.2$ sec meet the grid requirements. From Fig.17, the THD value of load voltage and load current for two level voltage source converter(VSC) using SPWM is 0.60% & 0.83% respectively.

4.2. Simulation results using SVPWM technique

The following figures represent the simulation results of SVPWM technique applied to DFIG based wind energy conversion system.

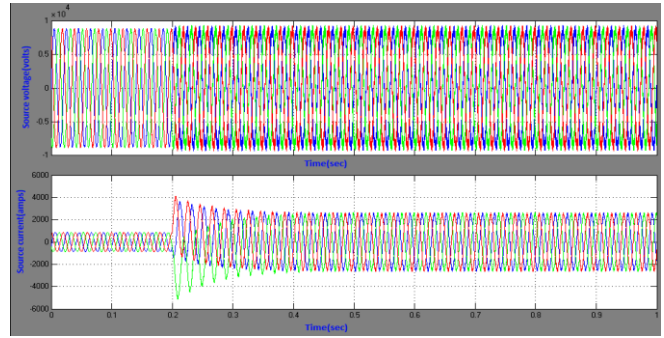


Fig 18. Source voltage and current of DFIG based WECS using SVPWM.

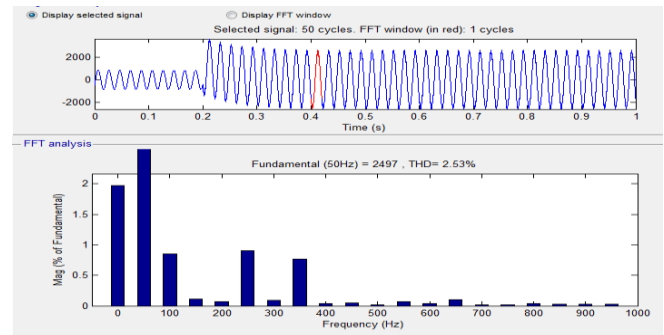
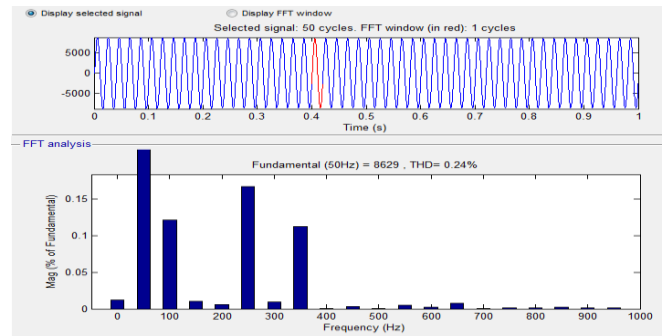


Fig 19. Source voltage and source current harmonic spectrum of two level VSC using SVPWM

The simulation result of Fig. 18 shows that, the voltage and current supplied by source. From Fig.19, the THD value of source voltage and source current for two level voltage source converter(VSC) using SVPWM is 0.24% & 2.53% respectively.

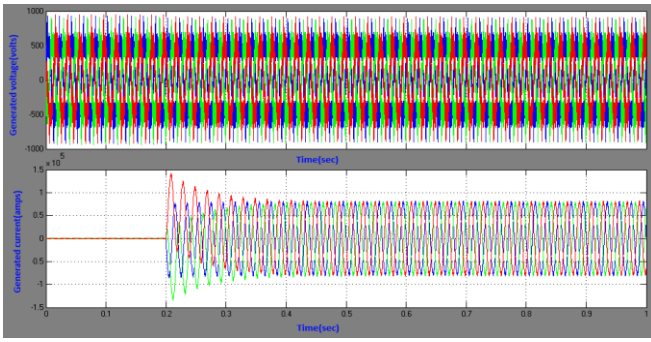


Fig 20.Generated voltage and current of DFIG

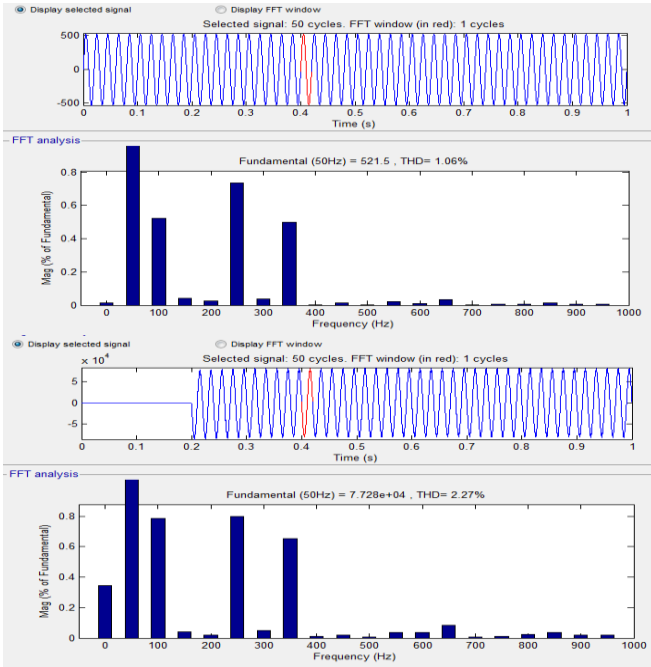


Fig 21.Generated voltage and current harmonic spectrum of two level VSC using SVPWM

The Fig .20 shows the voltage and current generated by the DFIG machine using SVPWM technique.The current upto $t = 0.2$ sec is zero as DFIG is not connected to the load. After $t = 0.2$ sec DFIG generates current to the load. From Fig.21, the THD value of generated volage and current for two level voltage souce converter(VSC) using SVPWM is 1.06% & 2.27% respectively.

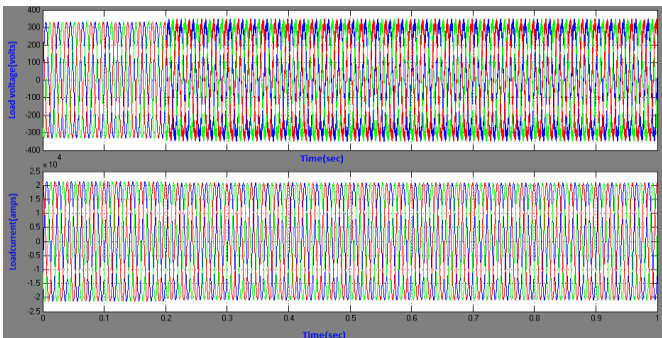


Fig 22. Load voltage and current of DFIG based WECS using SVPWM.

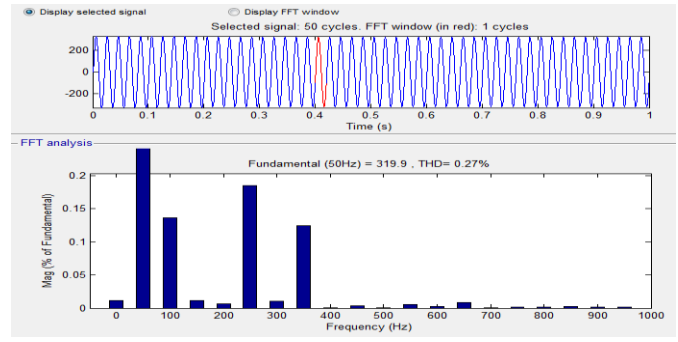


Fig 23.Load current harmonic spectrum of two level VSC using SVPWM

The Fig. 22 shows the voltage and current received by the load. Here the voltage and current after $t = 0.2$ sec meet the grid requirements. From Fig.23, the THD value of load voltage and current for two level voltage source converter (VSC) using SVPWM is 0.27% & 0.42% respectively.

Table 3. THD comparisons between SPWM and SVPWM

Parameters	SPWM	SVPWM
Source voltage	0.53	0.24
Source current	3.75	2.53
Generated voltage	2.15	1.06
Generated current	3.36	2.27
Load voltage	0.6	0.27
Load current	0.83	0.42

5. Conclusions

SVPWM is an optimum pulse width modulation technique for an inverter used in a variable frequency drive applications. SVPWM was originally developed as vector approach to Pulse Width Modulation Technique. Both SPWM and SVPWM techniques are used to provide controlled pulses to the gate terminals of the converter (rectifier/inverter) stations.

This paper presents the design and analysis of SPWM and SVPWM for two level converter employing DFIG based WECS are discussed. The SPWM and SVPWM control strategies for a two level Voltage Source converter (VSC) are implemented by using MATLAB/SIMULINK software. From the simulation study, the SVPWM gives the better quality i.e. lesser THD compared to SPWM.

Table. 4 Simulation Parameters of Wind Turbine

S.No	Characteristics	Value
1	Nominal Mechanical output power	1.5e6watts
2	Base wind speed	12 m/s
3	Pitch angle	7 deg
4	Base power of the electrical generator	1.5e6/0.9 VA
5	Maximun power at base wind speed	0.73
6	Base rotational speed	1.2

Table. 5 Simulation Parameters of DFIG

S.No	Characteristics	Value
1	Nominal power	1.5e6/0.9 VA
2	Voltage	415 V
3	Frequency	50Hz
4	Stator resistance	0.016 ohms
5	Stator, Rotor Inductance	0.06 henries
6	Rotor resistance	0.015 ohms
7	Mutual Inductance	3.5 henries

Table. 6 Simulation Parameters of Converter

S.No	Characteristics	Value
1	Switching Frequency	2KHz
2	Converter Frequency	50Hz
3	Modulation Index	0.89
4	Sample time	5e-6

References

- Arantxa Tapia, Gerardo Tapia, J. Xabier Ostolaza, and José Ramón Sáenz : Modeling and Control of a Wind Turbine Driven Doubly Fed Induction Generator. IEEE Transactions on Energy Conversion, Vol. 18, No. 2, June 2003.
- Ahmed G. Abo-Khalil, and Dong-Choon Lee, and Se-Hyun Lee: *Grid Connection of Doubly-Fed Induction Generators in Wind Energy Conversion System*. IEEE 5th International Conference on Power Electronics And Motion Control, 14-16 Aug. 2006.
- Mohsen Rahimi and Mostafa Parniani, Senior Member, IEEE: *Transient Performance Improvement of Wind Turbines with Doubly Fed Induction Generators Using Nonlinear Control Strategy*. IEEE Transactions on Energy Conversion, Vol. 25, No. 2, June 2010.
- Ghennam, T.Berkouk, E.M. Francois, B.: *Modeling and Control of a Doubly-Fed Induction Generator for Wind Turbine-Generator Systems*. International Conference on Power Engineering, Energy and Electrical Drives, 18-20 March 2009 published in IEEE Explore.
- El-Sattar, A.A.; Saad, N.H.; Shams El-Dein, M.Z: *Modeling and simulation of doubly fed induction generator variable speed wind turbine*. Power Systems Conference, 2006. MEPCON 2006, published in IEEE Explore.
- Ankit Gupta, S.N. Singh, Dheeraj K. Khatod: *Modeling and Simulation of Doubly Fed Induction Generator Coupled With Wind Turbine-An Overview*. Journal of Engineering, Computers & Applied Sciences ISSN No: 2319-5606 Volume 2, No.8, August 2013.
- J.G. Slootweg, H. Polinder, W.L. Klein: *Dynamic Modeling of a Wind Turbine with Doubly Fed Induction Generator*. 0-7803-7173-9/01/\$10.00 © 2001 IEEE.
- H. Abouobaida, M. Cherkaoui: *Modeling and Control of Doubly Fed Induction (DFIG) Wind energy conversion system*. Journal of Electrical Engineering, Volume 15 / 2015 - Edition: 1, Article 15.1.24.
- Sabir Messalti, Ahmed. Gherbi, Saad Belkhiat: *Improvement of Power System Transient Stability Using Wind Farms Based on a Doubly –Fed Induction Generation (DFIG)*. Journal of Electrical Engineering, Volume 13 / 2013 - Edition: 3, Article 13.3.24.
- Parminder Singh, Gagandeep Sharma, Sushil Prasher: *Power Control of DFIG Using Back to Back Converters (PWM Technique)*. International Journal of Engineering and Innovative Technology, Volume 3, Issue 3, September 2013.
- E. Hendawi, F. Khater and A. Shaltout: *Analysis, Simulation and Implementation of Space Vector Pulse Width Modulation Inverter*. Proceedings of the 9th WSEAS International Conference on Applications of Electrical Engineering.
- Avinash Mishra, Swaraj save, Rohit Sen: *Space Vector Pulse Width Modulation*. International Journal of Scientific & Engineering Research, Volume 5, Issue 2, February-2014.
- Lavanya Komma, Rangavalli Vasa: *Simulation and Comparison of Three Level Inverter Using SVPWM & SPWM*. International Journal of Electrical and Electronics Research ISSN 2348-6988 Vol. 2, Issue 3, pp: (21-30), Month: July - September 2014.
- K. Vinoth Kumar, Prawin Angel Michael, Joseph P. John and Dr. S. Suresh Kumar: *Simulation and Comparison of SPWM and SVPWM Control for Three Phase Inverter*. ARPN Journal of Engineering and Applied Sciences.

15. Y B Shukla and S K Joshi: *Space Vector Modulation for Three Phase Induction Dielectric Heating*. Journal of Electrical Engineering Volume 12 / 2012 - Edition: 4, Article 12.4.8.
16. Pradeep, J. and Devanathan, R.: *Comparative analysis and simulation of PWM and SVPWM inverter fed permanent magnet synchronous motor*. 3-15 Dec. 2012, published in IEEE Explore.